Biosensors and Bioelectronics 26 (2010) 748–753

Contents lists available at ScienceDirect

Biosensors and Bioelectronics

journal homepage: www.elsevier.com/locate/bios

Microbiosensors for glucose based on Prussian Blue modified carbon fiber electrodes for *in vivo* monitoring in the central nervous system

P. Salazar[a,*], M. Martín[a], R. Roche[a], J.L. González–Mora[a], R.D. O'Neill[b]

[a] Neurochemistry and Neuroimaging Group, Faculty of Medicine, University of La Laguna, Tenerife, Spain
[b] UCD School of Chemistry and Chemical Biology, University College Dublin, Belfield, Dublin 4, Ireland

ARTICLE INFO

Article history:
Received 9 April 2010
Received in revised form 4 June 2010
Accepted 25 June 2010
Available online 24 July 2010

Keywords:
Biosensor
Carbon fiber electrode
Glucose oxidase
Prussian Blue
Hydrogen peroxide
Poly(o-phenylenediamine)

ABSTRACT

Carbon fiber electrodes (CFEs) were used to develop microbiosensors for glucose as an alternative to the classical Pt and Pt–Ir transducers. Their low dimensions (~250 μm CFE length and ~10 μm diameter) are important factors for measurements in physiological environments. An electrocatalytic Prussian Blue (PB) film facilitated detection of enzyme-generated hydrogen peroxide at a low applied potential (~0.0 V against SCE), contrasting the high potential used in many previous designs (~0.7 V). The electrosynthesized polymer, poly-o-phenylenediamine (PoPD), was used to improve biosensor stability and selectivity against endogenous interference species, such as ascorbic and uric acids. Optimization of the fabrication procedure is described, including activation of CFE/PB, enzyme immobilization and stabilization, anti-interference films, optimizing applied potential, and pH effects. Analytical properties were also characterized such as sensitivity, LOD, linear range, and enzyme loading. Finally, an optimized biosensor displaying a linear sensitivity of 9.3 ± 0.1 μA mM^{-1} cm^{-2} ($n = 3$), a 2% RSD and free of interference, is proposed as a suitable candidate for *in vivo* glucose monitoring in the CNS.

© 2010 Elsevier B.V. All rights reserved.

1. Introduction

First generation biosensors are based on the detection of any electroactive metabolite that is generated (e.g., H_2O_2) or consumed (e.g., O_2) during the enzyme reaction. The principal problem of these approaches for oxidase-based biosensors is the high overpotential needed to detect either O_2 or H_2O_2 on Pt (Clark and Lyons, 1962; Clark, 1979) and other native electrode materials (Schuvailo et al., 2005). At high potentials, interference and polymerization reactions can occur at the biosensor surface. Biosensors in biological media are subject to interference by endogenous electroactive reducing agents, especially ascorbic acid (AA) and uric acid (UA) (D'Orazio, 2003; Osborne and Hashimoto, 2004; Garjonyte and Malinaus, 1999). These problems have been solved by several approaches: (a) the use of polymer films with anti-interference properties, such as poly-o-phenylenediamine (PoPD) (Lowry and O'Neill, 1994; Dai et al., 2006); (b) the use of artificial redox mediators (Castillo et al., 2003; Gregg and Heller, 1990; Habermüller et al., 2000; Mitala and Michael, 2006); (c) the use of electrocatalytic films to detect H_2O_2 at lower applied potentials (see Fig. 1) (Karyakin et al., 1995; Karyakin and Karyakina, 1999).

The neurophysiological motivation for this work is based on glucose being the principal source of energy in the brain. Fellows and Boutelle (1993) showed that physiological stimulation of neural activity is associated with an increase in glucose concentration in the extracellular compartment, which has a much longer duration than the associated change in regional cerebral blood flow (rCBF). On the other hand, recent studies suggest that increased energy requirements of activated neurons are met by neuronal utilization of lactate (Pellerin et al., 2007). Thanks to the development and use of microbiosensors to determine principal energy metabolites and neurotransmitters (Dale et al., 2005; Lowry et al., 1998), we can now further explore the relationship between neural activation, rCBF and brain metabolites.

Biosensors offer a variety of advantages over classical techniques for neurochemical monitoring: high spatial and temporal resolution; good selectivity; ease of implementation; amenable to miniaturization; rapid response time; etc. Recently, O'Neill et al. (2008) reviewed the development of wire-based amperometric polymer–enzyme composite biosensors, focusing on the relationship between key design features and analytical parameters. Using a carbon fiber substrate, we now propose a novel glucose biosensor, developed following this systematic approach, with significantly

* Corresponding author.
E-mail address: psalazar@ull.es (P. Salazar).

0956-5663/$ – see front matter © 2010 Elsevier B.V. All rights reserved.
doi:10.1016/j.bios.2010.06.045

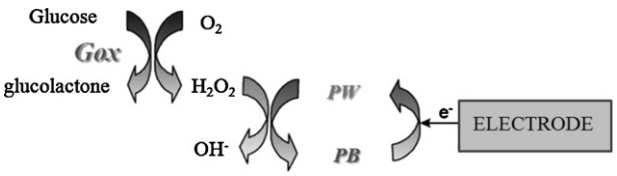

Fig. 1. Detection scheme for glucose biosensor based on a Prussian Blue (PB) modified electrode. Glucose is converted to gluconolactone, catalyzed by glucose oxidase (Gox) immobilized on the electrode surface. Secondary to this reaction is the production of hydrogen peroxide that can be reduced amperometrically at low applied overpotentials, electrocatalyzed by the PB.

smaller dimensions and a low working potential, which provide significant advantages for *in vivo* monitoring.

2. Materials and methods

2.1. Reagents and solutions

The enzyme glucose oxidase (Gox) from *Aspergillus niger* (EC 1.1.3.4, Type VII–S, lyophilized powder), glutaraldehyde (Glut, 25% solution) were obtained from Sigma Chemical Co., and stored at −21 °C until used. Other chemicals, including o-phenylenediamine (oPD), glucose, ascorbic acid (AA), uric acid (UA), polyethyleneimine (PEI), KCl, $FeCl_3$, $K_3[Fe(CN)_6]$, HCl (35%, w/w), H_2O_2 (30%, w/v), Nafion (5%, w/w, in a mixture of lower aliphatic alcohols and water), bovine serum albumin (BSA, fraction V) and phosphate buffer saline solution containing 0.1 M NaCl (PBS), were obtained from Sigma and used as supplied. PBS stock solutions (pH 7.4) were prepared in doubly distilled water (18.2 MΩ cm, Millipore–Q), and stored at 4 °C. Enzyme solutions were prepared in PBS, which also served as the background electrolyte for all *in vitro* experiments. Stock 1 M and 250 mM solutions of glucose were prepared in water, left for 24 h at room temperature to allow equilibration of the anomers, and stored at 4 °C. The PEI solutions used were prepared by dissolving PEI at 1% (w/v) and 5% (w/v) ratios in H_2O. The cross-linking solution was prepared in PBS with 1% (w/v) BSA and 0.1% (w/v) glutaraldehyde. Monomer solution of 300 mM oPD was prepared using 48.6 mg oPD and 7.5 mg BSA in 1.5 mL of N_2-saturated PBS and sonicating for 15 min. A 300 U/mL solution of Gox was prepared by dissolving 3.7 mg in 2 mL of PBS. Carbon fibers (8 μm diameter) were obtained from Goodfellow, glass capillaries from Word Precision Instruments Inc., 250 μm internal diameter Teflon-coated copper wire from RS, and silver epoxy paint was supplied by Sigma.

2.2. Instrumentation and software

Experiments were computer controlled with data acquisition software EChem™ for cyclic voltammetry and Chart™ for constant potential amperometry (ADInstruments Pty Ltd., Australia). The data acquisition system used was e–Corder 401 and a low-noise and high-sensitivity potentiostat, Picostat (eDAQ Pty Ltd., Australia). The linear and non-linear regression analyses were performed using the graphical software package Prism (ver. 5.00 GraphPad Software, San Diego, CA, USA). To electro-deposit and activate the PB (see Section 2.5), an in-house Ag/AgCl/saturated KCl reference electrode and platinum wire auxiliary electrode were used.

2.3. Amperometric experiments

All experiments were done in a 25 mL glass cell at 21 °C, using a standard three-electrode set-up with a commercial saturated calomel electrode (SCE) (CRISON Instrument S.A. Barcelona, Spain) as the reference and platinum wire as the auxiliary electrode. The applied potential chosen for most amperometric studies was 0.0 V against SCE. Glucose calibrations were performed in quiescent air-saturated PBS (following stabilization of the background current for 30 min) by adding aliquots of glucose stock solution (1 or 0.25 M) to the electrochemical cell. After the addition of glucose aliquots, the solutions were stirred for 10 s and then left to reach the quiescent steady-state current.

2.4. Data analysis

Calibration plots for glucose were generated by plotting averaged steady-state currents against substrate concentration and fitting the data, using non-linear regression to obtain the apparent Michaelis–Menten constants, K' (mM), maximum biosensor response, V_m (pA), and the Hill parameter, h. Linear regression was used in the linear range to determine biosensor sensitivity, signal to noise ratio and coefficient of determination (r^2). In all cases, the currents recorded in background electrolyte were subtracted from the calibration responses. Data are reported as mean ± SEM, n being the number of biosensors or number of measurements (as specified).

2.5. Preparation of the working electrodes

2.5.1. Fabrication of carbon fiber electrodes

Carbon fiber electrodes (CFEs) were constructed using the following steps. A carbon fiber (diameter 8 μm, 20–50 mm in length) was attached to Teflon-coated copper wire (diameter 250 μm)

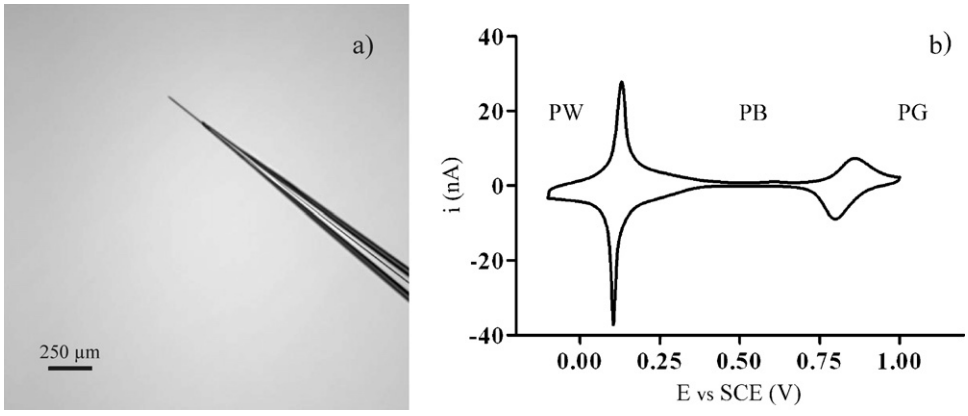

Fig. 2. a) Carbon fiber electrodes (CFEs) with a diameter of 8 μm and length of 250 μm. b) Cyclic voltammogram of the PB-modified CFE in de-aerated electrolyte solution (0.1 M KCl and 3 mM HCl) at a scan rate of 10 mV/s. PW is Prussian White, and PG is Prussian Green.

using high purity silver paint, and dried for 1 h at 80 °C. A borosilicate glass capillary was pulled to a tip using a vertical microelectrode puller (Needle/Pipette puller, Model 750, David Kopf Instruments, California, USA). After drying, the carbon fiber was carefully inserted into the pulled glass capillary tube under a microscope, leaving 2–4 mm of the carbon fiber protruding at the pulled end. Subsequently, the carbon fiber was cut to the desired length (approximately 250 μm), using a microsurgical scalpel. At the stem end of the capillary tube, the copper wire was fixed by casting with non-conducting epoxy glue; the carbon fiber was also sealed into the capillary mouth, using the same epoxy glue (Fig. 2a). Subsequently, CFEs were dried again for 1 h and were optically and electrochemically inspected before use.

2.5.2. PB electro-deposition onto carbon fiber electrodes

CFEs were modified by electro-deposition and activation of a Prussian Blue (PB) film. The PB layer was electro-deposited by a cyclic voltammetric (CV) method, applying *n* cyclic scans within the limits of −0.2 to 0.4 V, at a scan rate of 50 mV/s, to the CFEs in a fresh de-aerated solution containing 1.5 mM $K_3[Fe(CN)_6]$ and 1.5 mM $FeCl_3$ in 0.1 M KCl and 3 mM HCl. The electrode was then cleaned in doubly distilled water, and the CFE/PB activated by applying another *m* scans within the limits of −0.2 to 0.4 V at a scan rate of 100 mV/s in de-aerated electrolyte solution (0.1 M KCl and 3 mM HCl). Before being used, the CFE/PB was cleaned again in doubly distilled water for several seconds. Finally, the PB film was tempered at 100 °C for 2 h.

2.5.3. Microbiosensor construction based on CFE/PB

When modified Prussian Blue CFEs (CFE/PB) were ready to use, the next step was to immobilize the enzyme glucose oxidase (Gox). Gox was dissolved in PBS to the desired concentration (300 U/mL). Different methodologies to immobilize the enzyme were investigated to improve the analytical response (described in Section 3). After the immobilization step, all biosensors were cured for 1 h at 37 °C.

2.5.4. PoPD deposition onto the microbiosensors

Finally, an interference-rejection film of PoPD–BSA was electropolymerized onto the CFE/PB/Gox surface. Electrosynthesis of PoPD was carried out with a standard three-electrode set-up in PBS containing 300 mM oPD and 5 mg/mL of BSA, by applying a constant potential (+0.75 V) for 20–25 min. BSA was included in the monomer solution because globular proteins trapped in the PoPD polymer matrix can improve its permselectivity under some conditions (McAteer and O'Neill, 1996; Kirwan et al., 2007). For clarity in the nomenclature, however, the term BSA will be omitted in all sensor configurations, e.g., CFE/PB/Gox/PoPD.

After the biosensor fabrication procedure was completed, they were cleaned in doubly distilled water and stored overnight at 4 °C in a refrigerator, and used the next day. When not in use, biosensors were stored again at 4 °C in a refrigerator.

3. Results and discussion

3.1. Prussian Blue film

Prussian Blue (PB) has been widely used in biosensor construction to suppress or attenuate interference contributions (Li and Gu, 2006). Due to the peculiar structure of PB, its reduced form (Prussian White, PW) has a catalytic activity for H_2O_2 reduction in neutral media [*ec.1*], indirectly allowing H_2O_2 detection at potentials close to 0.0 V against SCE, and exhibiting better properties than other H_2O_2-detecting devices, such as Pt or horseradish peroxidase (Karyakin and Karyakina, 1999).

$$(PW)\,Fe_4K_4[Fe(CN)_6]_3 + 2H_2O_2 \rightarrow (PB)\,Fe_4[Fe(CN)_6]_3 + 4OH^- + 4K^+ \quad (1)$$

The zeolitic structure of PB with a cubic unit cell of 10.2 Å and with channel diameters of about 3.2 Å allows the diffusion of low molecular weight molecules (such as O_2 and H_2O_2) through the crystal structure (Ricci and Palleschi, 2005). A voltammogram of a PB-modified CFE is shown in Fig. 2b; two pairs of almost symmetrical peaks appear with formal potential values of ∼0.15 and ∼0.9 V, coinciding with formal potentials reported previously by others authors (Karyakin, 2001). The first peak pair corresponds to the interconversion of PW and PB, and the second pair from PB to Prussian Green (PG). Nevertheless, only the first peak pair will be studied; the response of this first peak pair points to a mono-electron, quasi-reversible process corresponding to a surface-adsorbed redox couple (Karyakin, 2001).

Due to this high activity and selectivity towards H_2O_2 reduction, some authors have named Prussian Blue an "artificial enzyme peroxidase" (Karyakin et al., 2000). Further improvements in the stability and selectivity of PB-based H_2O_2 transducers can be obtained by electropolymerizing a non-conducting PoPD permselective coating. Such improvements can increase 600-fold the selectivity of the PB/PoPD-based transducer relative to ascorbate, which is much better compared to the other reported systems (Lukachova et al., 2003; Salazar et al., in press).

3.2. Applied potential selection

To study the best operating potential, the effect of applied potential on the PB-modified electrode was studied in the range from −0.2 V to +0.2 V in PBS. The current generated by addition of 2.5 μM H_2O_2, was registered and represented as sensitivity in pA/μM. As can be seen in Fig. 3a the maximum response was obtained at 0.0 V, but no significant differences were found compared with other negative potentials; on the other hand, it was observed that sensitivity decreased rapidly at positive potential, giving significant differences between 0.0 V and +0.05 V ($p < 0.007$, $n = 3$), and complete loss of sensitivity at potentials close to +0.2 V. This observation can be justified on the basis that only the reduced form of PB (PW) possesses these electrocatalytic properties, so only at potentials where this form is present the electro-reduction of H_2O_2 can occur. This range of potentials is in agreement with the CV of the PB-modified CFE showed in Fig. 2b. Finally, 0.0 V was selected as the applied potential for glucose sensing.

3.3. Enzyme immobilization

3.3.1. Study of immobilization techniques

Glucose oxidase was immobilized on the transducer surface via dip-coating procedures. The principal problem of this method is the continuous loss of enzyme during the measurement process, due to the low strength of the non-specific interactions. To avoid this, enzyme can be attached to the surface by means of glutaraldehyde. The addition of another non-catalytic protein, with high numbers of lysine residues such us BSA, can help to diminish deactivation during the cross-linking phase and increase Gox stability (Gouda et al., 2001). The use of pre-casting with a polyelectrolyte, such as polyethyleneimine (PEI), has also been shown to stabilize and increase enzyme loading (Breccia et al., 2002; Qian et al., 2004).

To study how different methodologies of immobilization can improve the analytical properties of CFE/PB-based biosensors, several biosensor groups were developed. As a starting point, we used the following parameters in the electro-deposition of PB film: $n = 2$ and $m = 10$ to produce ∼10-μm diameter CFE/PB electrodes.

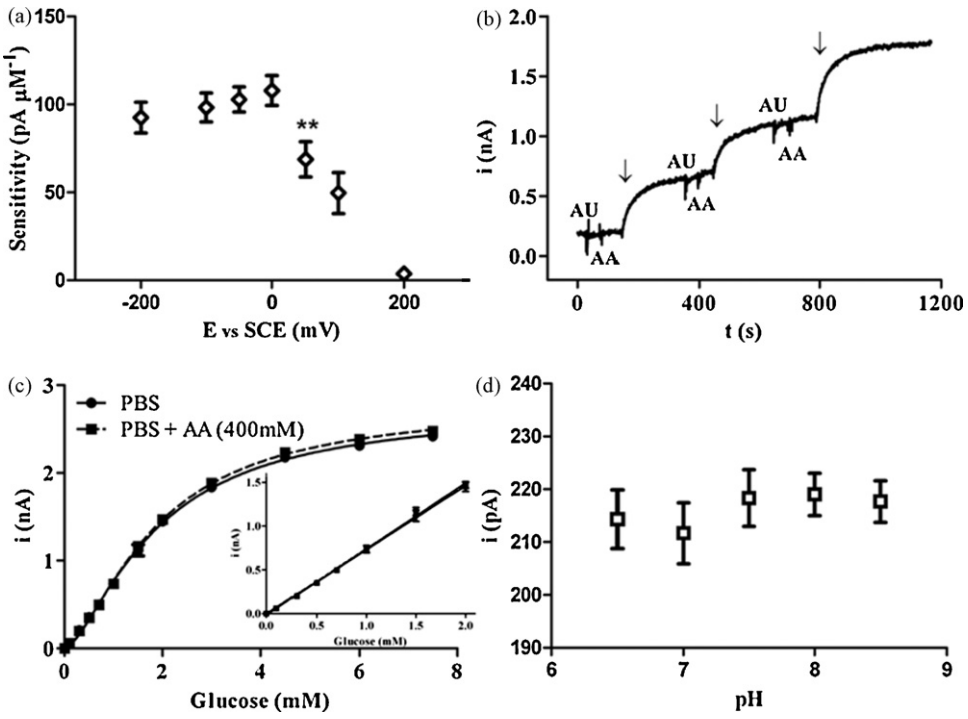

Fig. 3. a) Effect of the applied potential in the sensitivity of H_2O_2 in a PB-modified electrode in the studied range from −0.2 V to +0.2 V in PBS. b) Calibration raw data in PBS for optimized glucose biosensor with a PoPD film (CFE/PB/$PEI_{5\%}$/Gox_{opt}/PoPD): glucose additions of 1, 1 and 2 mM (arrows); and interference additions of 100 μM UA and 400 μM AA (current artifacts). c) Calibration curves of the optimized glucose biosensor in presence and absence of 400 μM of AA. d) Optimized glucose biosensor response to 0.5 mM addition of glucose in artificial extracellular fluid ECF adjusted at different pH values. Data are represented as mean ± SEM ($n = 3$).

Enzyme loading was modified by applying different immobilization protocols: (1) changing numbers of immersions (α) in Gox solution, and (2) the presence or absence of PEI in solutions before and during Gox immobilization.

The first group of CFE/PB microelectrodes were dip coated for 5 min to adsorb the enzyme (Gox) from the enzyme solution and finally cross-linked with glutaraldehyde (0.1%, w/v) and BSA (1%, w/v) (one fast immersion). This group was denoted by CFE/PB/Gox_0. The second and third groups were constructed in the similar way to the basic CFE/PB/Gox_0 design, but with additional α rapid immersions in enzyme and cross-linking solutions, waiting 5 min between each dip-evaporation cycle. Accordingly, this fabrication procedure, for which $\alpha = 5$ or 10, provided biosensors of the form: CFE/PB/Gox_5 and CFE/PB/Gox_{10}.

A fourth group of biosensors were constructed using the same protocol of CFE/PB/Gox_5, but adding an additional solution (1% PEI). The biosensors were dipped briefly in this PEI solution after the enzyme solution and before cross-linking solution. According to this fabrication procedure, the biosensors produced were: CFE/PB/$(Gox–PEI_{1\%})_5$. A fifth group of biosensors were constructed using the same protocol as CFE/PB/$(Gox–PEI_{1\%})_5$, but after stabilizing the PB film and before enzyme immobilization, biosensors were dipped in a 5% PEI solution and dried for 1 h. In this case the nomenclature was: CFE/PB/$PEI_{5\%}$/$(Gox–PEI_{1\%})_5$. The last group of biosensors were constructed using the same protocol as for CFE/PB/$PEI_{5\%}$/$(Gox–PEI_{1\%})_5$, but using 5% PEI for all PEI applications. In this case the nomenclature selected was: CFE/PB/$PEI_{5\%}$/$(Gox–PEI_{5\%})_5$.

Table 1 shows the enzyme kinetic and analytical parameters obtained from calibration curves for different ∼10-μm diameter glucose biosensors fabricated with and without PEI and different deposition procedures. These results show that increased numbers of dip-coatings increased the relative active enzyme loading (increasing V_m) and linear range sensitivity. Increasing the amount of PEI also increased sensitivity significantly. The value of apparent Michaelis constant (K') for the basic configuration (CFE/PB/Gox_0, 20–30 mM) was close to the value reported for free enzyme (Swoboda and Massay, 1965), indicating that immobilization on PB had no detrimental effect on enzyme affinity. The incorporation of PEI increased enzyme affinity, which was the main mechanism for enhanced linear sensitivity ($\sim V_m/K'$ (O'Neill et al., 2008)), leading to lower LOD values. Almost all biosensors showed hyperbolic behavior (Hill parameter, $h \approx 1$), except the last 'basic' design, where $h \approx 2$ (sigmoidal behavior) making it unsuitable for straightforward glucose monitoring applications.

When the number of deep-coatings is increased, the biosensor manufacturing time suffers a considerable increase. So the final fabrication process (*developed below*) was optimized with respect to time. Several configurations of PB deposition, activation steps and enzyme immobilization were studied (data not shown) to optimize the balance of glucose sensitivity and fabrication time. The most important fabrication parameters selected, following systematic optimization, are summarized as follows:

(1) *PB deposition*: $n = 3$, PB activation: $m = 50$ and stabilization for 2 h at 100 °C.
(2) *Enzyme immobilization*: one fast immersion in 5% PEI and dried for 1 h; one immersion in Gox (300 U/mL) and drying period (5 min for each step); 30 fast immersions in Gox solution, and finally, 15 fast immersions in cross-linking solution (BSA/Glut).

This microbiosensor design will be referred to as: CFE/PB/$PEI_{5\%}$/Gox_{opt} (see enzyme and analytical parameters in Table 1)

3.3.2. Study of poly-o-phenylenediamine anti-interference film

At the low applied potential used in the present work, the influence of physiological interferences on the response of the biosensor should be very low. One useful way in diminishing this electroactive interference further, and also improve the stability

Table 1
Enzyme kinetic and analytical parameters of different glucose biosensor designs.

Biosensors	Sensitivity (pA/mM)	r^2 in L.R.	Detection Limit (μM)	K' (mM)	V_m (pA)	h
CFE/PB/Gox_0	10.0 ± 0.3	0.999	564	27 ± 3	339 ± 33	0.9 ± 0.1
CFE/PB/Gox_5	20.3 ± 1.3	0.984	270	19 ± 3	643 ± 68	0.9 ± 0.1
CFE/PB/Gox_{10}	38.5 ± 1.3	0.996	103	19 ± 2	1240 ± 128	0.8 ± 0.1
CFE/PB/$(Gox–PEI_{1\%})_5$	74.8 ± 2.7	0.997	57	13 ± 2	1306 ± 42	1.1 ± 0.1
CFE/PB/$PEI_{5\%}/(Gox–PEI_{1\%})_5$	111 ± 7	0.991	47	10.3 ± 1.5	1661 ± 55	1.2 ± 0.1
CFE/PB/$PEI_{5\%}/(Gox–PEI_{5\%})_5$	523 ± 5	0.999	10	3.2 ± 0.6	1967 ± 41	2.0 ± 0.2
CFE/PB/$PEI_{5\%}/Gox_{opt}$	1814 ± 29	0.999	3	1.7 ± 0.2	5300 ± 57	1.6 ± 0.1
CFE/PB/$PEI_{5\%}/Gox_{opt}$/PoPD	747 ± 7	0.999	8	2.6 ± 0.1	2790 ± 20	1.4 ± 0.1

Mean ± SEM (n = 3 biosensors) for: linear sensitivity, coefficient of determination; and apparent Michaelis constant (K') and calibration plateau (V_m; see Fig. 3). Detection limit was calculated as 3 × SD of the background current. The Hill parameter is included to highlight possible deviations from straightforward Michaelis–Menten kinetics, for which h = 1. Calibration curves were obtained by applying 0.0 V against SCE in air-saturated PBS (pH 7.4).

of the PB film, is to employ permselective films (Salazar et al., in press). These films minimize access of interference species and exclude surface-active macromolecules (Lyne and O'Neill, 1990). Among these electropolymerized films are PoPD and analogues, polyphenol, and overoxidized polypyrrole (Basudam Adhikari and Majumdar, 2004; Yuqing et al., 2004). The self-controlling film thickness of PoPD during electropolymerization, reproducibly provides a thin and uniform film thickness (3–15 nm) (Killoran and O'Neill, 2008; Rothwell et al., 2008). The use of BSA can increase the interference rejecting properties of the PoPD (McAteer and O'Neill, 1996; Ryan et al., 1997; Dixon et al., 2002; Kirwan et al., 2007).

PoPD films were grown potentiostatically on the CFE/PB/$PEI_{5\%}/Gox_{opt}$ surface at +0.75 V against Ag/AgCl. After electropolymerization, biosensors were rinsed with distilled water and allowed to dry for approximately 1 h before being used. The PoPD film reduced the biosensor sensitivity to glucose by ~40–50% compared with the PoPD-free CFE/PB/$PEI_{5\%}/Gox_{opt}$ design (see Table 1). Nevertheless, the sensitivity of CFE/PB/$PEI_{5\%}/Gox_{opt}$/PoPD was 0.75 nA/mM corresponding to a current density of 9.3 ± 0.1 μA mM^{-1} cm^{-2} (n = 3). This was due to a combination of significantly higher V_m and lower K' values compared with the non-optimized designs; see Table 1. Biosensor responses to glucose (1 mM), with and without 400 μM AA (principal physiological interference), were recorded and normalized as a percentage with respect to current observed without AA. No significant differences were found in the absence (100 ± 2%) and presence of 400 μM AA (99 ± 3%, n = 5, p > 0.66).

Fig. 3b and c show calibration data for glucose and the effect of two principal endogenous brain interference species, using CFE/PB/$PEI_{5\%}/Gox_{opt}$/PoPD. In Fig. 3b several additions of AA (400 μM) and UA (100 μM) had no effect on either the background current or on the sensitivity of biosensor when glucose concentration was increased by 1, 1 and 2 mM, respectively. No significant difference was found in the entire glucose calibration plot (Fig. 3c), and specifically the linear sensitivity of the optimized biosensor design (Fig. 3c, *inset*) in the absence (737 ± 7 pA/mM) and presence (756 ± 14 pA/mM) of AA (400 μM), p > 0.23, n = 8. These results indicate that the effects of electroactive interference, at low applied potentials and using PoPD as permselective films, are negligible and suggest that these devices might be suitable for monitoring a complex matrix like CNS tissue.

3.3.3. pH dependence

pH plays an important role in affecting the sensitivity of glucose biosensors, because both the bioactivity of Gox and the stability of the PB film are pH dependent. It is clearly reported that PB is unstable and dissolves at pH values above 7 (Feldman and Murray, 1987), suggesting an important problem when working in physiological media. One way to solve these problems is by using a polyelectrolyte, such as PEI, to reduce possible changes in enzyme conformation by the formation of cationic–anionic complexes, and an external polymer film (PoPD) to increase the stability of the PB layer. The effect of pH of the detection solution on the response of optimized glucose biosensor (CFE/PB/$PEI_{5\%}/Gox_{opt}$/PoPD) was investigated using artificial extracellular fluid ECF (135 mM NaCl, 3 mM KCl, 1 mM $MgCl_2$, 1.2 mM $CaCl_2$) in a pH range from 6.5 to 8.5. Fig. 3d shows no significant changes in the glucose response at different pH values, confirm the excellent stability of the devices, and shows that Gox and PB are well stabilized on the CFE surface.

3.4. In vivo recording

In order to demonstrate that glucose biosensors based on CFE/PB respond to changes in glucose levels in brain extracellular fluid (ECF), we examined the effect of local injection of glucose and depolarization with 150 mM KCl on responses recorded with (CFE/PB/$PEI_{5\%}/Gox_{opt}$/PoPD) in the ECF; all experiments were done after reaching the baseline (~30 min). Fig. 4 shows changes of glucose registered in prefrontal cortex after local injections of 2 mM glucose via a micro-pipette on the surface exposed of the cortex in the proximity of the biosensor: (a) 1 μL; (b) 0.5 μL and (c) 0.1 μL at an injection flux of 3 μL min^{-1}. Clear biosensor response changes during infusion are evident and, after the first injection, the glucose levels remained augmented (upper inset). Linear correlation appears between glucose change and volume injected (r^2 = 0.97), i.e., no saturation effect was observed.

Spreading depression (SD) is a striking and highly reproducible response of the gray matter of the CNS. Normoxic SD can be triggered by high-frequency electrical pulses and a variety of chemicals. Among the chemical agents noteworthy are potassium ions

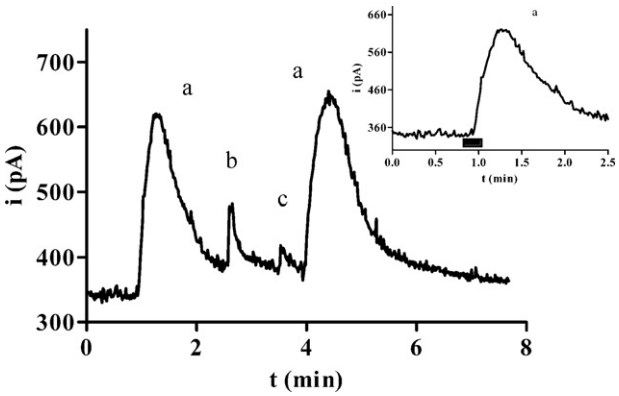

Fig. 4. Raw current changes of glucose microbiosensor recorded with the optimized configuration (CFE/PB/$PEI_{5\%}/Gox_{opt}$/PoPD) in brain extracellular fluid after local injections of 2 mM glucose (PBS, pH 7.4 100 mM NaCl) in an anesthetized Sprague Dawley rat: (a) 1 μL; (b) 0.5 μL and (c) 0.1 μL at injection flux of 3 μL min^{-1}. Upper inset represents the first peak where the injection period is denoted with a black bar.

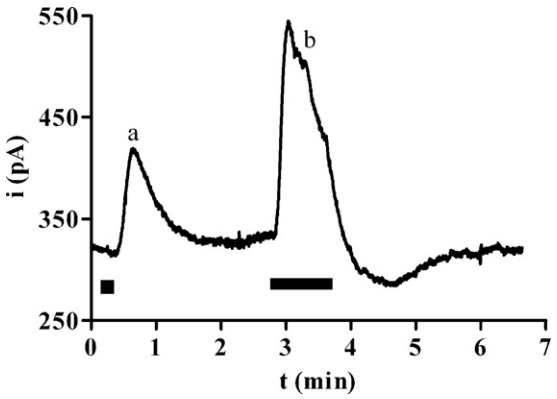

Fig. 5. Raw current changes of glucose microbiosensor recorded with the optimized configuration (CFE/PB/$PEI_{5\%}$/Gox_{opt}/PoPD): response in brain extracellular fluid after several transient of spreading depression generated by injection of 150 mM KCl in PBS in anesthetized Sprague Dawley rat. Injection flux 5 μL min^{-1}: a) volume injected 1 μL; b) volume injected 5 μL.

and glutamate. In our case a single SD episode was elicited by applying an aliquot of 150 mM KCl in PBS to the surface of the cortex beside the implanted biosensor. Biosensor responses associated with different volume injections of KCl are shown in Fig. 5, where a clear increase in current (dose dependent) was observed after different KCl injections. This was followed by a slower restoration of the basal levels, especially for the last injection where the volume injected was 5 μL and the time to reach basal levels, after terminating local injection, was estimated to be ~2 min. After each experiment, the sensitivity of the biosensors did not show significant changes, demonstrating its good anti-biofouling properties.

4. Conclusions

Microbiosensors of glucose based on PB-modified CFEs have been developed. Several advantages of this approach were: small dimensions, low applied potentials (associated with electrocatalysis by the PB deposit) and anti-interference properties (due to low applied potential and a PoPD permselectivity film), and these have been contrasted to conventional Pt–Ir-based biosensors (higher dimensions and potentials) for work in physiological media. Principal steps of fabrication have also been discussed: electrodeposition and activation of CFE with PB, enzyme immobilization, etc. By exploring enzyme immobilization steps, biosensors with different analytical properties have been developed. Optimal applied potential studies for H_2O_2 detection, and pH effects on biosensor response have also been investigated and discussed. Finally, an optimized biosensor configuration, CFE/PB/$PEI_{5\%}$/Gox_{opt}/PoPD, is proposed as an effective candidate to be used for *in vivo* studies with a sensitivity of 9.3 ± 0.1 μA mM^{-1} cm^{-2} ($n = 3$), RSD of 2% and free of electroactive interference.

Acknowledgements

The funds for the development of this device have been provided by the following national public projects: ULLAPD-08/01 granted by the Agencia Canaria de Investigación, Innovación y Sociedad de la Información, Ministerio de Industria, Turismo y Comercio (Proyecto AVANZA) TSI-020100-2008-337 and Ministerio de Ciencia e Innovación (Proyecto CICYT) TIN2008-06867-C02-01/TIN.

References

Basudam Adhikari, B., Majumdar, S., 2004. Prog. Polym. Sci. 29 (7), 699–766.
Breccia, J.D., Andersson, M.M., Hatti–Kaul, R., 2002. Biochim. et Biophys. Acta 1570 (3), 165–173.
Castillo, J., Gáspár, S., Sakharov, I., Csöregi, E., 2003. Biosens. Bioelectron. 18 (5–6), 705–714.
Clark Jr., L.C., 1979. Methods in Enzymology, vol. 56. Academic Press, New York.
Clark Jr., L.C., Lyons, C., 1962. Ann. N. Y. Acad. Sci. 102, 29–45.
Dai, Y.Q., Zhou, D.M., Shiu, K.K., 2006. Electrochim. Acta 52 (1), 297–303.
Dale, D., Hatz, S., Tian, F., Llaudet, E., 2005. Trends Biotechnol. 23 (8), 420–428.
Dixon, B.M., Lowry, J.P., O'Neill, R.D., 2002. J. Neurosci. Methods 119, 135–142.
D'Orazio, P., 2003. Clin. Chim. Acta 334 (1–2), 41–69.
Feldman, B.J., Murray, R.W., 1987. Inorg. Chem. 26 (11), 1702–1708.
Fellows, L.K., Boutelle, M.G., 1993. Brain Res. 604 (1–2), 225–231.
Garjonyte, R., Malinaus, A., 1999. Sens. Actuators B 56 (1–2), 85–92.
Gouda, M.D., Thakur, Karanth, N.G., 2001. Electroanalysis 13 (10), 849–855.
Gregg, B.A., Heller, A., 1990. Anal. Chem. 62 (3), 258–263.
Habermüller, K., Mosbach, M., Schuhmann, W., 2000. Fresenius J. Anal. Chem 366 (6–7), 560–568.
Karyakin, A.A., 2001. Electroanalysis 13 (10), 813–819.
Karyakin, A.A., Gitelmacher, O.V., Karyakina, E.E., 1995. Anal. Chem. 67 (14), 2419–2423.
Karyakin, A.A., Karyakina, E.E., 1999. Sens. Actuators B 57 (1–3), 268–273.
Karyakin, A.A., Karyakina, E.E., Gordon, L., 2000. Anal. Chem. 72 (7), 1720–1723.
Killoran, S.J., O'Neill, R.D., 2008. Electrochim. Acta 53 (24), 7303–7312.
Kirwan, S.M., Rocchitta, G., McMahon, C.P., Craig, J.D., Killoran, S.J., O'Brien, K.B., Serra, P.A., Lowry, J.P., O'Neill, R.D., 2007. Sensors 7 (4), 420–437.
Li, J.P., Gu, H.N., 2006. J. Chin. Chem. Soc. 53 (3), 575–582.
Lowry, J.P., Miele, M., O'Neill, R.D., Boutelle, M.G., Fillenz, M., 1998. J. Neurosci. Methods 79 (1), 65–74.
Lowry, J.P., O'Neill, R.D., 1994. Electroanalysis 6 (5–6), 369–379.
Lukachova, L.V., Kotel'nikova, E.A., D'Ottavi, D., Shkerin, E.A., Karyakina, E.E., Moscone, D., Palleschi, G., Curulli, A., Karyakin, A.A., 2003. IEEE Sens. J. 03 (3), 326–332.
Lyne, P.D., O'Neill, R.D., 1990. Anal. Chem. 62 (21), 2347–2351.
McAteer, K., O'Neill, R.D., 1996. Analyst 121 (6), 773–777.
Mitala, J.J., Michael, A.C., 2006. Anal. Chim. Acta 556 (2), 326–332.
O'Neill, R.D., Lowry, J.P., Rocchitta, G., McMahon, C.P., Serra, P.A., 2008. Trends Anal. Chem. 27 (1), 78–88.
Osborne, P., Hashimoto, M., 2004. Analyst 129, 759–765.
Pellerin, L., Bouzier–Sore, A.K., Aubert, A., Serres, S., Merle, M., Costalat, R., Magistretti, P.J., 2007. Glia 55 (12), 1251–1262.
Qian, J.M., Suo, A.L., Yao, Y., Jina, Z.H., 2004. Clin. Biochem. 37 (2), 155–161.
Ryan, M.R., Lowry, J.P., O'Neill, R.D., 1997. Analyst 122 (11), 1419–1424.
Ricci, F., Palleschi, G., 2005. Biosens. Bioelectron. 21 (3), 389–407.
Rothwell, S.A., Killoran, S.J., Neville, E.M., Crotty, A.M., O'Neill, R.D., 2008. Electrochem. Commun. 10 (7), 1078–1081.
Salazar P., Martín M., Roche R., O'Neill R.D., González-Mora J.L., Electrochim. Acta, in press, doi:10.1016/j.electacta.2010.06.036.
Schuvailo, O.N., Dzyadevych, S.V., El'skaya, A., Gautier-Sauvigne, S., Csoregi, E., Cespuglio, R., Soldatkin, A.P., 2005. Biosens. Bioelectron. 21 (1), 87–94.
Swoboda, B.E.P., Massay, V., 1965. J. Biol. Chem. 240 (5), 2209–2215.
Yuqing, M., Jianrong, C., Xiaohua, W., 2004. Trends Biotechnol. 22 (5), 227–231.